Extrinsic origin of the insulating behavior of polygrain icosahedral Al-Pd-Re quasicrystals

J. Dolinšek,[1] P. J. McGuiness,[1] M. Klanjšek,[1] I. Smiljanić,[2] A. Smontara,[2] E. S. Zijlstra,[3] S. K. Bose,[4] I. R. Fisher,[5] M. J. Kramer,[6] and P. C. Canfield[6]

[1]*J. Stefan Institute, University of Ljubljana, Jamova 39, SI-1000 Ljubljana, Slovenia*

[2]*Institute of Physics, Bijenička 46, POB 304, HR-10001 Zagreb, Croatia*

[3]*Theoretische Physik, Universität Kassel, D-34132 Kassel, Germany*

[4]*Department of Physics, Brock University, St. Catharines, Ontario, Canada L2S 3A1*

[5]*Geballe Laboratory for Advanced Materials and Department of Applied Physics, Stanford University, California 94035-4045, USA*

[6]*Ames Laboratory and Department of Physics and Astronomy, Iowa State University, Ames, Iowa 50011, USA*

(Received 21 April 2006; revised manuscript received 27 June 2006; published 3 October 2006)

Polygrain icosahedral *i*-Al-Pd-Re quasicrystals are known to exhibit dramatically different electronic transport properties to other Al-based quasicrystals. By performing comparative experimental and theoretical studies of the electronic transport and electronic structure of polygrain and monocrystalline *i*-Al-Pd-Re samples, we show that the extraordinarily high electrical resistivity and the metal-to-insulator transition in the polygrain material are not intrinsic properties of the quasiperiodic lattice, but are of extrinsic origin due to the high porosity and the oxygen-rich weakly insulating regions in the material. We also compare theoretical electronic structures and experimental electrical resistivities of monocrystalline *i*-Al-Pd-Re and *i*-Al-Pd-Mn quasicrystals and show that there are no significant differences between these two isomorphous compounds, suggesting that *i*-Al-Pd-Re is on common ground with other Al-based quasicrystals. We present a structural model of *i*-Al-Pd-Re.

DOI: 10.1103/PhysRevB.74.134201 PACS number(s): 61.44.Br, 71.23.Ft

Based on numerous experimental studies of cast and annealed polygrain material,[1–13] the electronic transport properties of icosahedral *i*-Al-Pd-Re quasicrystals (QCs) are considered to be dramatically different to any other known quasicrystalline compound. The low-temperature resistivity $\rho_{4.2\ \mathrm{K}}$ is of the order $0.1-1\ \Omega\,\mathrm{cm}$ and the resistivity increase ratio from room temperature (RT) to 4.2 K, $R=\rho_{4.2\ \mathrm{K}}/\rho_{300\ \mathrm{K}}$, is by a factor of up to 200 or more, both figures being by far the highest among known QCs. The large negative-temperature-coefficient (NTC) resistivity and the extraordinarily high $\rho_{4.2\ \mathrm{K}}$ values, not expected for an alloy of regular metals, suggest that *i*-Al-Pd-Re may be semiconductorlike, undergoing a metal-to-insulator transition (MIT) at low temperature.[2] This is in contrast to the semimetallic behavior of other related Al-rich icosahedral phases in Al-Cu-Fe, Al-Cu-Ru, Al-Cu-Os, Al-Cu-Cr, and Al-Pd-Mn, which all exhibit $\rho_{4.2\ \mathrm{K}}$ values in the range[14] $2-10\ \mathrm{m}\Omega\,\mathrm{cm}$ and small resistivity-increase factors $R=1.4-2.5$, i.e., a factor of about 100 smaller than *i*-Al-Pd-Re. Such large differences are surprising from the atomic- and electronic structure points of view. Though no exact structural model of the icosahedral phase in *i*-Al-Pd-Re is available as yet, there exists strong evidence that its structure is similar to the well-studied *i*-Al-Pd-Mn, involving an isomorphous substitution of Mn by the isoelectronic Re. The x-ray diffraction pattern of *i*-Al-Pd-Re can be exactly deduced from that of *i*-Al-Pd-Mn, providing that the six-dimensional unit-cell parameter is slightly inflated[13] (from $a_6=6.452$ Å in *i*-Al-Pd-Mn to $a_6=6.53$ Å in *i*-Al-Pd-Re), accounting for the larger atomic radius of Re compared to that of Mn. In addition, the ideal icosahedral compositions of both compounds are about the same, i.e., $Al_{70.5}Pd_{21}Mn(Re)_{8.5}$. Based on powder x-ray diffraction (where detailed differences in the structural perfection and compositional fluctuations are indistinguishable), many investigated polygrain *i*-Al-Pd-Re samples were reported to be of high structural quality, so that their extraordinarily high resistivity and insulating behavior at low temperatures were considered to be a genuine intrinsic property of a perfect quasiperiodic structure. However, though prepared by the same method, different polygrain *i*-Al-Pd-Re samples of the same or similar nominal composition exhibited a large scatter of the resistivity values, by as much as 50 times,[11] and the increase in the factor *R* varied between 3 and 200. The polygrain samples were produced in an arc furnace under argon or helium. The samples were then annealed in vacuum under optimal conditions[3] (12 h @ 940 °C) and rapidly quenched in chilled water. The samples that underwent this kind of treatment exhibited the resistivity-increase factors *R* up to 20. It was reported[3] that there exists another temperature region, below which further annealing can lead to a large increase in $\rho_{4.2\ \mathrm{K}}$ and the *R* factor. The extreme $\rho_{4.2\ \mathrm{K}}\approx 1\ \Omega\,\mathrm{cm}$ and $R\approx 200$ values, comparable to those observed in doped semiconductors well inside the insulating region of the MIT,[15] were obtained for samples subject to a two-step annealing (typically 12 h @ 940 °C followed by 10 h @ 600 °C). A metallurgical study has reported that polygrain *i*-Al-Pd-Re has a high porosity.[16]

In 2000, Guo *et al.*[17] synthesized the first large *i*-Al-Pd-Re single crystals of composition $Al_{71.7}Pd_{19.4}Re_{8.9}$ by a slow-cooling method and further investigations were made on as-grown (not annealed) material. The samples showed a high degree of structural perfection over a long range. Surprisingly, the 300 K electrical resistivity of the single crystals was measured to be only $2-4\ \mathrm{m}\Omega\,\mathrm{cm}$ and $\rho_{2\ \mathrm{K}}\approx 3-6\ \mathrm{m}\Omega\,\mathrm{cm}$, with the *R* increase being less than 2. This is by a factor of about 100 smaller than for the polygrain samples, but in the same range as for all other Al-based icosahedral QCs.[14] Using a similar technique, by slow cooling a prealloyed melt from 1025 to 900 °C, large single

i-Al-Pd-Re QCs were also grown by Fisher *et al.*[18] These crystals were annealed at 900 °C for several days *in* the melt prior to decanting (annealing *outside* the melt resulted in partial decomposition) and showed a high degree of structural order and a minimal phason content. In agreement with Guo *et al.*'s electrical resistivity results,[17] the resistivity of the single *i*-QC samples with a varying Al-to-Pd content exhibited values $\rho_{2\ \mathrm{K}}=2-7\ \mathrm{m\Omega\,cm}$ and the resistivity increase $\rho_{1.8\ \mathrm{K}}/\rho_{300\ \mathrm{K}}=1.2-2.5$. These figures suggest that *i*-Al-Pd-Re is on common ground with other Al-based QCs, raising the question as to what is the genuine intrinsic electrical transport in a perfect quasiperiodic lattice—semimetalliclike, as typically found in all Al-based QC families except polygrain *i*-Al-Pd-Re; or semiconductorlike, with a MIT at low temperature observed in polygrain *i*-Al-Pd-Re?

In order to answer this question, we performed a comparative experimental and theoretical study of the electronic transport properties of the *i*-Al-Pd-Re material in both the polygrain and the single-crystalline forms. We used representative material including the extreme cases of an insulating polygrain sample with $\rho_{4\ \mathrm{K}}$ as large as 3 Ω cm and a low-resistivity monocrystal with $\rho_{4\ \mathrm{K}}\approx 3.5\ \mathrm{m\Omega\,cm}$. In addition, we compared the electronic properties of *i*-Al-Pd-Re and *i*-Al-Pd-Mn flux-grown monocrystalline samples.

The polygrain *i*-Al-Pd-Re sample was produced by arc melting according to the procedure described in detail in Ref. 3. The sample with a nominal icosahedral composition $Al_{70.5}Pd_{21}Re_{8.5}$ underwent a two-step annealing (12 h @ 940 °C and 10 h @ 600 °C). Its electrical resistivity $\rho(T)$ is shown in Fig. 1(a), whereas the conductivity $\sigma=1/\rho$, together with the fit $\sigma=\sigma_0+aT^{\alpha}$ [using $\sigma_0=8.6\times10^{-2}\ \Omega^{-1}\ \mathrm{cm}^{-1}$, $a=2.3\times10^{-2}\ \Omega^{-1}\ \mathrm{cm}^{-1}$ (assuming dimensionless temperature) and $\alpha=1.35$], is shown in Fig. 1(b). The RT resistivity amounts to $\rho_{300\ \mathrm{K}}=19.9\ \mathrm{m\Omega\,cm}$, whereas $\rho_{4.2\ \mathrm{K}}=3.07\ \Omega\,\mathrm{cm}$, making $R=154$. The thermoelectric power [the Seebeck coefficient $S(T)$] is shown in Fig. 1(c). The thermopower is large, amounting to $S_{300\ \mathrm{K}}=84\ \mu\mathrm{V/K}$, and positive, suggesting the diffusivity of positively charged carriers. The large $\rho_{4.2\ \mathrm{K}}$ and R values indicate that this sample is, at low temperatures, on the insulating side of the MIT (considered to occur at $\rho\approx 1\ \Omega\,\mathrm{cm}$), whereas the large thermopower is also characteristic of semiconductors.

For the single crystal we used a sample of composition $Al_{73.5}Pd_{17.1}Re_{9.4}$, and the details of its growth and characterization are described in Ref. 18. The sample was annealed for 3 days at 900 °C *in* the melt and then decanted. Its $\rho(T)$ is shown in Fig. 1(a), indicating $\rho_{300\ \mathrm{K}}=1.9\ \mathrm{m\Omega\,cm}$, $\rho_{4.2\ \mathrm{K}}=2.7\ \mathrm{m\Omega\,cm}$ and $R=1.4$. The thermopower is small [Fig. 1(c)], amounting to $S_{300\ \mathrm{K}}=-7\ \mu\mathrm{V/K}$, and negative, indicating electron diffusivity. These $\rho(T)$ and $S(T)$ values are about the same as found in other Al-based icosahedral QCs that are considered to be semimetals. Therefore, based on the electrical resistivity and the thermopower, the investigated polygrain and monocrystalline *i*-Al-Pd-Re samples appear profoundly different. Here it is important to stress that $\rho(T)$ and $S(T)$ are long-range transport quantities, where the charge carriers are traveling over macroscopic distances in the material.

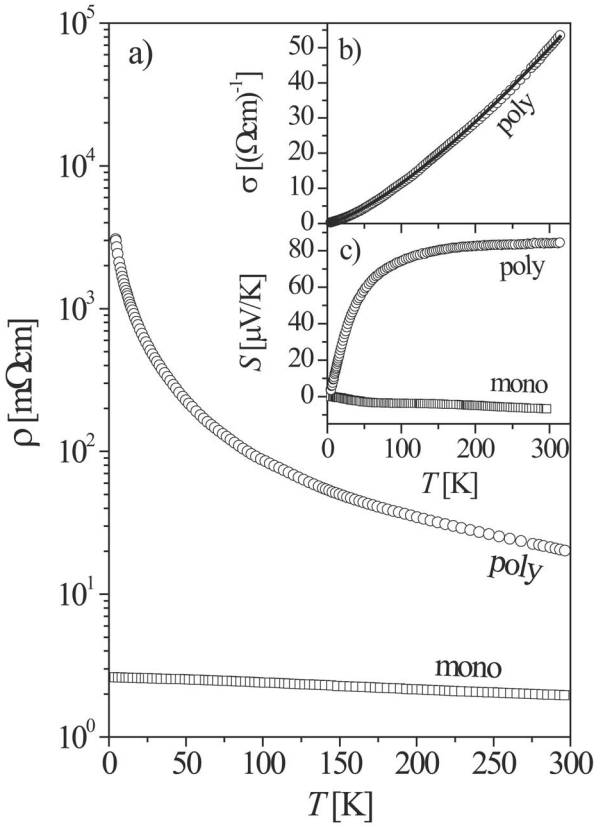

FIG. 1. (a) Electrical resistivities ρ of the polygrain and monocrystalline *i*-Al-Pd-Re. (b) Electrical conductivity $\sigma=\rho^{-1}$ of the polygrain sample (solid line is the fit $\sigma=\sigma_0+aT^{1.35}$). (c) Thermopowers [Seebeck coefficient $S(T)$] of the two samples.

It is tempting to see whether this large difference could originate from the difference in the electronic density of states (DOS) at the Fermi energy E_F between the two samples. An experimental check is provided by measuring the ^{27}Al NMR spin-lattice relaxation rate T_1^{-1}, where the nuclear spins are relaxed via coupling to the conduction electrons. The relaxation rate depends[19] on the square of the DOS at E_F, $T_1^{-1}\propto g^2(E_F)$, and is sensitive to the *local* (site specific) DOS around the resonant Al atoms under the condition of no net electrical current (i.e., in the absence of long-range electron transport). The relaxation rates of the investigated polygrain and monocrystalline samples between 400 and 4 K are shown in Fig. 2(a) in a $(T_1T)^{-1}$ vs T plot. The electronic origin of the relaxation rate was confirmed by observing the field-independence of T_1^{-1} (measured in two magnetic fields 2.35 T and 4.7 T) down to the lowest temperature. The equality of the relaxation mechanisms in both samples is evident from the inset in Fig. 2(a), where the ^{27}Al magnetization-recovery curves of the two samples (displayed on a normalized time scale τ/T_1, where the variable delay τ of the pulsed experiment at a given temperature is scaled to the respective T_1 value in order to remove temperature dependence) perfectly overlap at high (200 K) and low (20 K) temperatures. Disregarding the details of the temperature dependence of $(T_1T)^{-1}$ (which can be found in Ref. 19), the main result of the NMR relaxation experiment is the fact that the $(T_1T)^{-1}$'s of the two samples exhibit only minor differ-

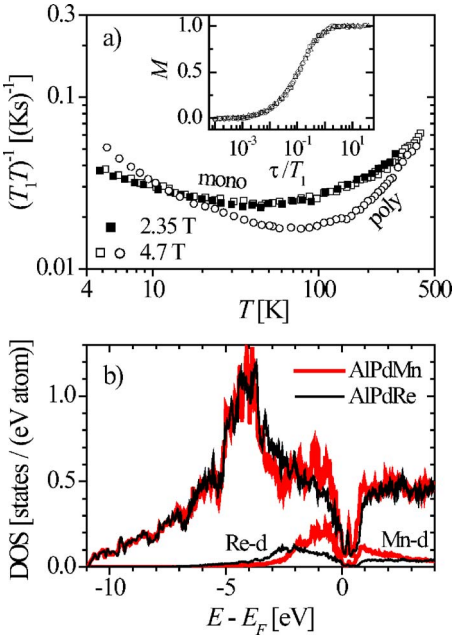

FIG. 2. (Color online) (a) ^{27}Al NMR spin-lattice relaxation rate of the polygrain and monocrystalline *i*-Al-Pd-Re. The inset shows the ^{27}Al magnetization-recovery curves on a normalized time scale τ/T_1 at 200 K and 20 K of both samples superimposed. (b) Electronic DOSs of the Al-Pd-Mn and Al-Pd-Re theoretical quasicrystalline approximants. The lower curves show the partial Re-*d* and Mn-*d* contributions.

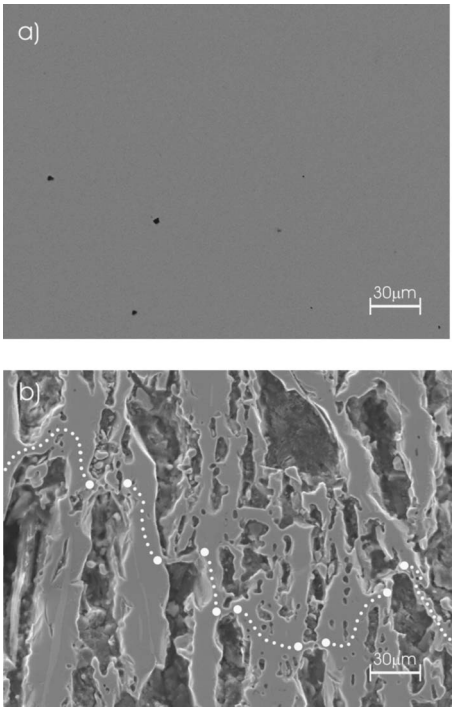

FIG. 3. Secondary-electron images of (a) monocrystalline and (b) polygrain *i*-Al-Pd-Re. A connected pathway through the porous geometry of the polygrain sample is indicated in (b) by a dotted line (the bridges are located between the large dots).

ence, having the ratio $(T_1T)^{-1}_{poly}/(T_1T)^{-1}_{mono}=0.65$ at $T=80$ K, where the difference is the largest. Since $(T_1T)^{-1} \propto g^2(E_F)$, this yields an estimate $g(E_F)_{poly}/g(E_F)_{mono}=0.81$, so that the local DOSs at the Al sites of the investigated samples are about the same and cannot be the origin of the large difference in the resistivity and the thermopower.

To get a theoretical insight into the DOS, we performed a comparative *ab initio* study of the DOSs of the isomorphous $Al_{70.8}Pd_{21.5}Mn_{7.7}$ and $Al_{70.8}Pd_{21.5}Re_{7.7}$ using the fully relaxed Quandt-Elser periodic approximant model that in the past has efficiently reproduced the photoemission spectra of these QCs.[20] The details of the DOS calculation, performed with the WIEN2k computer program, are given in the Appendix (where a structural model of *i*-Al-Pd-Re is presented also), and the resulting total DOSs of the isostructural Al-Pd-Mn and Al-Pd-Re theoretical QC approximants are displayed in Fig. 2(b). The partial Re-*d* and Mn-*d* DOSs are also shown. We observe that the DOSs of both compounds at low energies follow approximately the square-root dependence of a free-electronlike DOS. This is due to the mainly Al-character of the wave functions at these energies. The energy region between 5 and 3.5 eV below E_F is dominated by Pd-*d* states. The resulting peaks do not differ significantly between *i*-Al-Pd-Mn and *i*-Al-Pd-Re. The main difference between the two compounds is that the Re-*d* states contribute to the DOS over a wider energy range below E_F than the Mn-*d* states. Similarly the Mn-*d* contribution to the DOS above the pseudogap is more pronounced. This leads to a somewhat wider pseudogap in *i*-Al-Pd-Re and to a more gradual, less abrupt decrease of the DOS when going from the Pd-*d* peak to the pseudogap around E_F. In spite of these differences, the DOSs of *i*-Al-Pd-Mn and *i*-Al-Pd-Re exhibit a very similar pseudogap and DOS values at E_F, suggesting that the electronic properties of both compounds should not differ significantly. Consequently, the DOS cannot account for the extraordinarily large NTC resistivity and thermopower of the polygrain *i*-Al-Pd-Re.

The origin of the difference between the investigated polygrain and monocrystalline *i*-Al-Pd-Re samples becomes evident by performing a thorough structural characterization of the samples. SEM secondary electron (SE) images of the polished surfaces of the two samples are shown in Fig. 3. While the monocrystal is a bulk homogeneous material, exhibiting only a few remote small pores [Fig. 3(a)], the polycrystal is a highly porous material, exhibiting an irregular fractal-like geometry [Fig. 3(b)]. Long-range transport in such a geometry is a percolation problem: in order to travel from one end of the sample to the other, the electron must find a connected pathway through a labyrinth of bulky "islands" connected by bridges. In Fig. 3(b) we indicated one possible connected path from the left to the right end of the specimen. The electrons must travel over tiny bridges in order to reach the other islands (the same applies in a three-dimensional matrix). In an electrical resistivity (and thermopower) experiment, the sample's effective cross section for the electron transport in the fractal geometry of Fig. 3(b) is strongly reduced, which can account for the high resistivity of the polygrain sample. However, the porous structure by itself is not sufficient to introduce the large NTC resistivity increase R upon cooling.

The origin of the spectacularly large R becomes evident when analyzing *locally* the composition of the islands and

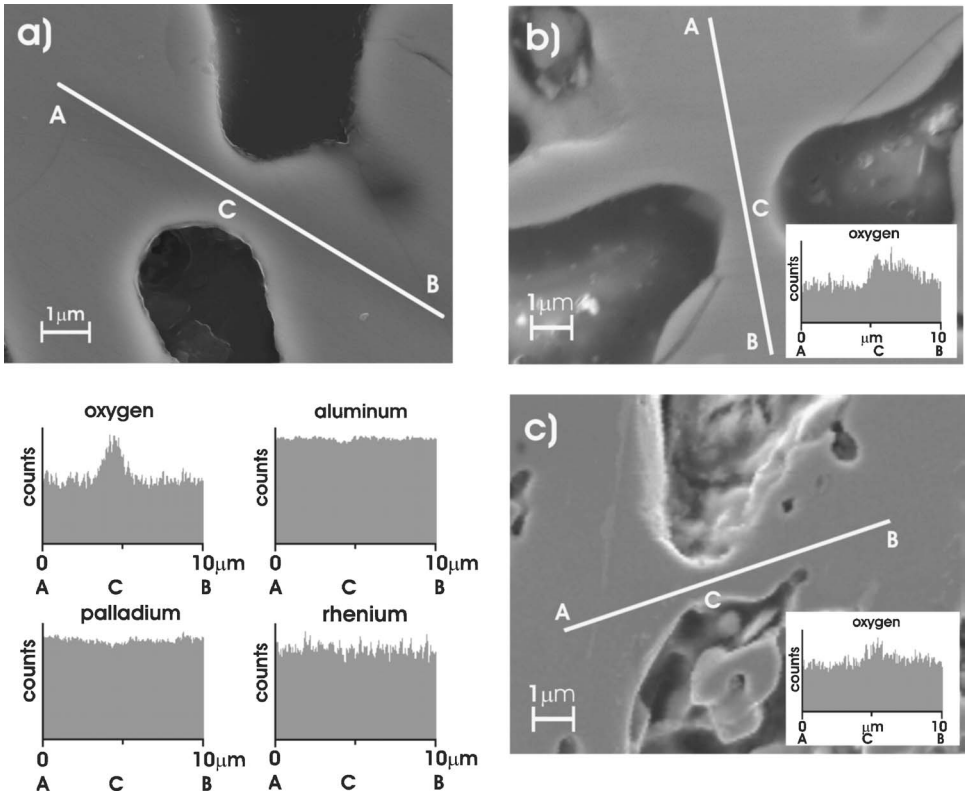

FIG. 4. Secondary-electron images of three representative bridges [(a), (b), and (c)] in the porous structure of the polygrain *i*-Al-Pd-Re. The concentration line profiles of the constituent elements over the bridges are also shown.

bridges using energy-dispersive x-ray spectroscopy (EDXS). We used a JEOL JSM-6500F SEM with an analyzed subsurface volume of 0.6 μm diameter, which was small enough to determine the composition within the bridges (of typical width 1.5 μm or more). By performing line profiles of the concentrations of the constituent elements over the bridges, we detected a significant concentration of *oxygen*, in addition to Al, Pd, and Re. A representative example is displayed in Fig. 4(a). By quantitatively analyzing points on the line profile, we found at both ends (located in islands), in at. %, $Al_{64.5}Pd_{23.6}Re_{8.5}O_{3.4}$ at point *A* and $Al_{64.6}Pd_{22.9}Re_{8.6}O_{3.9}$ at point *B*, which can be considered the same within the experimental uncertainty (0.5%). In the middle of the bridge (point *C*) we found $Al_{61.9}Pd_{22.0}Re_{8.1}O_{8.0}$, so that the oxygen content within the bridge is significantly increased by a factor 2.2 with respect to the bulk. The line profiles of the individual elements O, Al, Pd, and Re are also displayed in the panel of Fig. 4(a), showing an increase of O and depletion of Al, Pd, and Re within the bridge. The oxygen-concentration line profiles of two other bridges are shown in Figs. 4(b) and 4(c), where the oxygen increase in the bridge of Fig. 4(b) is by a factor 1.9, and in Fig. 4(c) by a factor of about 1.5. The oxygen enrichment thus varies randomly depending on the bridge. In contrast, the EDXS analysis of the monocrystal at three random spots on the surface of Fig. 3(a) gave the average concentration $Al_{68.8}Pd_{18.2}Re_{10.9}O_{2.1}$ with the standard deviation ±0.3. This oxygen content is significantly lower than that detected in the polycrystal and represents the background concentration near the surface.

As oxidized material is generally more electrically insulating, the oxygen-rich bridges represent a kind of weakly insulating junction between more conducting regions of the material, acting as potential barriers through which electrons must penetrate in order to establish the long-range conductivity. The random geometry of the porous matrix of polygrain *i*-Al-Pd-Re and the random oxygen enrichment within the bridges introduce a random distribution of potential barriers. At temperatures not close to $T=0$, crossing the barriers will be thermally activated. At low temperatures, the electrons are confined to certain regions of the material, whereas at elevated temperatures they start to migrate over the sequence of barriers and become more extended. A semiconductorlike behavior and a MIT can clearly be imagined in such a system. The investigated polygrain *i*-Al-Pd-Re thus resembles a doped semiconductor and, more closely, systems with variable-range hopping conductivity. However, this behavior does not originate from the quasiperiodicity, but from the specific form of the porous and oxidized material. Since high porosity was independently observed in other polygrain *i*-Al-Pd-Re samples,[16] it would not be surprising if this conclusion also applies to the polygrain samples used in other studies. In addition, different degrees of porosity and oxidation of the material (the latter is very likely attained during the annealing process) offer simple explanation to the reported puzzle[11] why different polygrain *i*-Al-Pd-Re samples of the same or similar nominal composition, and prepared by the same method, exhibit such a large scatter of the resistivity values (by as much as 50 times) and *R* factors (between 3 and 200). High resistivity, semiconductorlike behavior, and the MIT of the polygrain *i*-Al-Pd-Re do not appear to be related to the quasiperodicity.

Finally, it is worth commenting on the possible origin of the high porosity of polygrain *i*-Al-Pd-Re samples. Though a definite answer is still pending, the reason is very likely met-

allurgical: in Al-Pd-Re, the melting temperature of Re (3180 °C) is much higher from the melting temperatures of Al (660 °C) and Pd (1554 °C). In contrast, Mn (1246 °C) in Al-Pd-Mn is much closer to the other two elements [similarly, Al-Cu-Fe QCs involve Cu (1083 °C) and Fe (1538 °C) in addition to Al]. Alloying elements with so much different melting temperatures as in Al-Pd-Re may have side effects. This is supported by the annealing experiments on the *i*-Al-Pd-Re monocrystalline samples,[18] where annealing outside the melt resulted in partial decomposition of the material.

We thank S. J. Poon for provision of the polygrain *i*-Al-Pd-Re sample and for reading the manuscript prior to submission and I. Tudosa (Stanford) for help with synthesis of the monocrystalline *i*-Al-Pd-Re and *i*-Al-Pd-Mn samples. Ames Laboratory is operated for the U.S. Department of Energy by Iowa State University under Contract No. W-7405-ENG-82. This work was supported by the Director of Energy Research, Office of Basic Energy Sciences. I.R.F. acknowledges support from the NSF, Grant No. DMR-0134613. E.S.Z. and S.K.B. acknowledge financial support from the Natural Sciences and Engineering Research Council of Canada. Calculations were performed on computers of SHARCNET (Hamilton, Canada).

APPENDIX

The calculation of the DOS starts from the Quandt-Elser (QE) structural model[21] of *i*-Al-Pd-Mn, which is a hypothetical periodic approximant, corresponding to composition $Al_{70.8}Pd_{21.5}Mn_{7.7}$ (that is close to the ideal icosahedral composition). The QE model is composed of the same atomic clusters as the ideal *i*-Al-Pd-Mn QCs, namely Bergman and Mackay-like clusters. Following the original QE model that was relaxed using the Γ point,[21] this model has been recently modified[22] by breaking the symmetry (from space group *Immm* to *Cm*) and relaxing the structure further using 8 special **k** points (some of which were equivalent), which has led to a lowering of the total energy by 0.029 eV/atom. Here we shall only consider this latter modified model and use it for comparison of the electronic structures of *i*-Al-Pd-Mn and *i*-Al-Pd-Re.

The details of calculation for the *i*-$Al_{70.8}Pd_{21.5}Mn_{7.7}$, together with the atomic coordinates and the lattice parameters, are given in the previous paper.[22] The same calculation was conducted also for the *i*-$Al_{70.8}Pd_{21.5}Re_{7.7}$ by replacing Mn by the isoelectronic Re. The atomic coordinates and the lattice parameters of *i*-Al-Pd-Re were relaxed in the same way as those of *i*-Al-Pd-Mn using the ABINIT pseudopotential computer program[23] with the only exception that a plane-wave cutoff energy for the wave functions of 600 eV turned out to be sufficient for the *i*-Al-Pd-Re alloy, while plane waves with energies up to 800 eV were needed for *i*-Al-Pd-Mn. The optimized lattice parameters of *i*-$Al_{70.8}Pd_{21.5}Re_{7.7}$ were obtained as $a=7.75$, $b=12.55$, and $c=20.44$ Å, which are on average 1.4% larger than those of *i*-Al-Pd-Mn[22] (where $a=7.65$, $b=12.50$, and $c=20.14$ Å), reflecting the fact that Re is larger than Mn. The optimized angle γ between the lattice vectors **a** and **b** was obtained as 89.7°, which is very close to the optimized value of 89.9° that we have found for *i*-Al-Pd-Mn.[22] The optimized atomic coordinates of the *i*-$Al_{70.8}Pd_{21.5}Re_{7.7}$ structural model are given in Table I and the unit cell is displayed in Fig. 5. Most of the atoms in *i*-Al-Pd-Re did not move far (typically less than 0.1–0.2 Å) from their initial positions in the model of *i*-Al-Pd-Mn. We found that the smallest Al-Re distance (2.43 Å) in *i*-Al-Pd-Re was larger than the smallest Al-Mn distance (2.33 Å) in *i*-Al-Pd-Mn, which is not surprising due to the

TABLE I. Optimized atomic coordinates expressed as fractions of the lattice vectors **a**, **b**, and **c** of *i*-$Al_{70.8}Pd_{21.5}Re_{7.7}$. [The coordinates are given according to the convention of Ref. 33, space group *Cm* (No. 8), unique axis c, cell choice 3.]

Class	Site	$x(a)$	$y(b)$	$z(c)$
Al0a	4b	−0.005	0.308	0.246
Al0b	4b	−0.003	−0.319	0.245
Al1a	4b	−0.013	0.681	0.621
Al1b	4b	−0.005	−0.690	0.618
Al2a	4b	0.678	−0.005	0.697
Al2b	4b	−0.688	−0.007	0.694
Al3a	4b	0.325	0.001	0.079
Al3b	4b	−0.324	0.001	0.081
Al4a	4b	0.195	0.103	0.200
Al4b	4b	0.193	−0.118	0.194
Al4c	4b	−0.197	0.107	0.194
Al4d	4b	−0.201	−0.117	0.193
Al5	2a	0.126	0.484	0
Al6	2a	−0.009	0.049	0
Al7a	4b	0.313	−0.370	0.067
Al7b	4b	−0.305	−0.389	0.065
Al7c	4b	0.488	0.422	0.115
Al7d	2a	0.350	0.309	0
Al7e	2a	−0.244	0.408	0
Al8a	4b	0.153	0.185	0.085
Al8b	4b	0.158	−0.178	0.067
Al8c	4b	−0.206	0.201	0.071
Al8d	4b	−0.179	−0.184	0.067
Al9a	4b	−0.002	0.373	0.115
Al9b	4b	0	−0.375	0.119
Pd0	4b	−0.005	−0.009	0.730
Pd1a	2a	0.509	0.121	0
Pd1b	2a	0.503	−0.114	0
Pd2a	4b	0.284	0.300	0.188
Pd2b	4b	0.287	−0.311	0.187
Pd2c	4b	−0.296	0.301	0.184
Pd2d	4b	−0.291	−0.312	0.182
Pd3	4b	−0.004	0.495	0.307
Re0a	2a	0.009	0.295	0
Re0b	2a	−0.002	−0.320	0
Re1	4b	−0.001	−0.005	0.117
Re2	2a	0.480	0.498	0

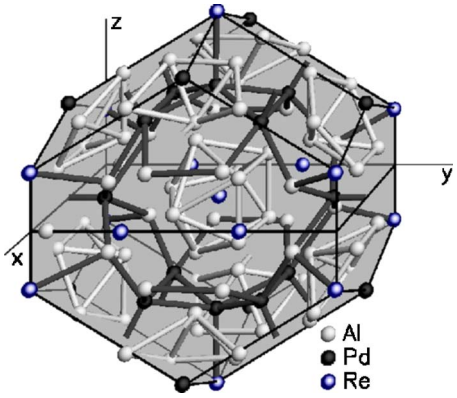

FIG. 5. (Color online) Unit cell of the structural model of i-$Al_{70.8}Pd_{21.5}Re_{7.7}$. Selected bonds are shown to emphasize the geometrical structure. Light bonds indicate the first shell of a Mackay-like cluster (in the center of the unit cell) and the first shells (icosahedra) of two Bergman clusters. Dark bonds indicate the second shells (pentagonal dodecahedra) of the Bergman clusters.

larger Re size. Presumably for the same reason the largest displacement was obtained for $A16$, which is located near the origin of the coordinate system in Fig. 5: it moved 0.5 Å in the y direction, thus increasing its distance to the Re1 atoms above and below. The result that some atoms in the i-Al-Pd-Re structure are significantly shifted with respect to the positions in the i-Al-Pd-Mn has also been found experimentally by Yamamoto *et al.*[24] in an x-ray diffraction study of i-$Al_{73}Pd_{18}Re_9$. Moreover, they found that some atomic sites in the i-$Al_{71}Pd_{21}Mn_8$ reference structure remain unoccupied in the i-$Al_{73}Pd_{18}Re_9$, a fact that is not taken into account in our calculations.

The electronic DOSs of i-Al-Pd-Mn and i-Al-Pd-Re were calculated with the full-potential linearized augmented-plane-wave computer program WIEN2k.[25] This program is based on density functional theory.[26] The electronic exchange and correlation energy was treated within the local-density approximation.[27] Our basis consisted of plane waves with energies less than or equal to 116 and 90 eV for i-Al-Pd-Mn and i-Al-Pd-Re, respectively. Inside the muffin-tin spheres around each atom the plane waves were augmented by atomic orbitals with a linearized energy dependence. To get a better convergence with respect to the number of plane waves included in the calculation, the transition-metal d states were described with a combination[28] of energy-independent augmented plane waves and local orbitals. The radii of the muffin-tin spheres were chosen to be 1.10 Å for the spheres around the Al atoms and 1.23 Å for the spheres around the transition metals Pd and Mn in the calculation for the i-Al-Pd-Mn. In i-Al-Pd-Re, the muffin-tin radii were 1.13 Å for the Al atoms and 1.30 Å for Pd and Re. To enforce orthogonality of the high-lying semicore states to the valence states, we treated the Pd-4p, Mn-3p, Re-5p, and Re-4f semicore states as valence states using local orbitals.[29] The calculated electronic DOSs of isomorphous i-$Al_{70.8}Pd_{21.5}Mn_{7.7}$ and i-$Al_{70.8}Pd_{21.5}Re_{7.7}$ are compared in Fig. 2(b), suggesting that the electronic properties of both QCs should be of the same order of magnitude.

In Fig. 6 we compare experimental electrical resistivities $\rho(T)$ of two monocrystalline icosahedral samples of nominal

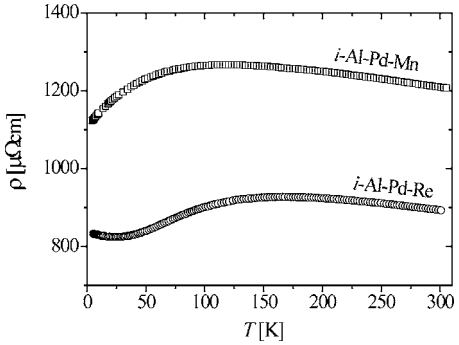

FIG. 6. Electrical resistivities of flux-grown monocrystalline i-$Al_{72}Pd_{19.5}Mn_{8.5}$ (squares) and i-$Al_{74}Pd_{17}Re_9$ (circles) quasicrystals.

compositions i-$Al_{72}Pd_{19.5}Mn_{8.5}$ and i-$Al_{74}Pd_{17}Re_9$ (this i-Al-Pd-Re monocrystalline sample is from another batch, but from the same origin as before), both grown by the self-flux technique. The details of preparation and characterization of i-$Al_{72}Pd_{19.5}Mn_{8.5}$ are reported in Ref. 30. Its resistivity is in the range $\rho \approx 1200\ \mu\Omega$ cm and exhibits a broad maximum at about 120 K. This kind of temperature dependence is typically observed in i-Al-Pd-Mn QCs, which usually exhibit a maximum somewhere between RT and 4 K and sometimes also a minimum at still lower temperatures.[30] The resistivity of i-$Al_{74}Pd_{17}Re_9$ is not much different both in magnitude ($\rho \approx 900\ \mu\Omega$ cm) and the temperature dependence by exhibiting a maximum around 150 K and a shallow minimum at about 20 K. Electrical conductivity (the inverse resistivity) of a metallic material generally depends on a product of the electronic DOS at E_F and the electronic diffusion constant D. Assuming isomorphic character of the i-Al-Pd-Mn and i-Al-Pd-Re structures and comparable structural quality of the two investigated samples (both coming from the same crystal-growing source), it is reasonable to assume that the electronic diffusion constants in the two compounds are not much different. The qualitative and quantitative similarity of the i-Al-Pd-Mn and i-Al-Pd-Re resistivities as shown in Fig. 6 thus supports our prediction that the DOSs of the two compounds are only marginally different, so that electrical transport in i-Al-Pd-Mn and i-Al-Pd-Re should be basically the same. This is another hint that i-Al-Pd-Re is on common ground with other Al-based QCs.

It is interesting to note that Krajčí and Hafner[31] have reached the opposite conclusion based on calculations that were aimed at explaining the high resistivity of polygrain i-Al-Pd-Re samples. Using Katz and Gratias' model, they have demonstrated theoretically that the DOS of the 1/1 approximant of composition $Al_{68.8}Pd_{15.6}Re_{15.6}$ exhibits a pseudogap of width 0.15 eV just below E_F, whereas there is no counterpart of this phenomenon in the isostructural $Al_{68.8}Pd_{15.6}Mn_{15.6}$. On this basis they suggested that high-quality i-Al-Pd-Re QCs are semiconductors with a low density of localized states inside the gap. A more recent study[32] by the same authors predicts that the above-mentioned $Al_{68.8}Pd_{15.6}Re_{15.6}$ 1/1 approximant is a member of a class of 27 semiconducting 1/1 approximants. Figure 2(b) shows that our study based on the QE models of i-$Al_{70.8}Pd_{21.5}Mn_{7.7}$ and i-$Al_{70.8}Pd_{21.5}Re_{7.7}$ does not reproduce these results.

[1] H. Akiyama, Y. Honda, T. Hashimoto, K. Edagawa, and S. Takeuchi, Jpn. J. Appl. Phys., Part 1 **32**, L1003 (1993).
[2] F. S. Pierce, S. J. Poon, and Q. Guo, Science **261**, 737 (1993).
[3] F. S. Pierce, Q. Guo, and S. J. Poon, Phys. Rev. Lett. **73**, 2220 (1994).
[4] Q. Guo, F. S. Pierce, and S. J. Poon, Phys. Rev. B **52**, 3286 (1995).
[5] P. Lindqvist, P. Lanco, C. Berger, A. G. M. Jansen, and F. Cyrot-Lackmann, Phys. Rev. B **51**, 4796 (1995).
[6] S. J. Poon, F. S. Pierce, and Q. Guo, Phys. Rev. B **51**, 2777 (1995).
[7] Q. Guo and S. J. Poon, Phys. Rev. B **54**, 12793 (1996).
[8] M. Ahlgren, C. Gignoux, M. Rodmar, C. Berger, and Ö. Rapp, Phys. Rev. B **55**, R11915 (1997).
[9] A. D. Bianchi, F. Bommeli, M. A. Chernikov, U. Gubler, L. Degiorgi, and H. R. Ott, Phys. Rev. B **55**, 5730 (1997).
[10] J. Delahaye, J. P. Brison, and C. Berger, Phys. Rev. Lett. **81**, 4204 (1998).
[11] J. Delahaye, C. Gignoux, T. Schaub, C. Berger, T. Grenet, A. Sulpice, J. J. Prejean, and J. C. Lasjaunias, J. Non-Cryst. Solids **250-252**, 878 (1999).
[12] M. Rodmar, M. Ahlgren, D. Oberschmidt, C. Gignoux, J. Delahaye, C. Berger, S. J. Poon, and Ö. Rapp, Phys. Rev. B **61**, 3936 (2000).
[13] J. J. Préjean, J. C. Lasjaunias, C. Berger, and A. Sulpice, Phys. Rev. B **61**, 9356 (2000).
[14] See, for a review, Ö. Rapp, in *Physical Properties of Quasicrystals*, edited by Z. M. Stadnik, Springer Series in Solid-State Sciences, Vol. 126 (Springer, Berlin, 1999), p. 127 (see Tables 5.1. and 5.2. and references therein).
[15] See, e.g., T. G. Castner, in *Hopping Transport in Solids*, edited by M. Pollak and B. Shklovskii, Modern Problems in Condensed Matter Sciences, Vol. 28 (North-Holland, Amsterdam, 1991), p. 1.
[16] K. Kirihara and K. Kimura, *Quasicrystals*, Mater. Res. Soc. Symp. Proc. **553**, 379 (1999).
[17] J. Q. Guo, T. J. Sato, E. Abe, H. Takakura, and A. P. Tsai, Philos. Mag. Lett. **80**, 495 (2000).
[18] I. R. Fisher, X. P. Xie, I. Tudosa, C. W. Gao, C. Song, P. C. Canfield, A. Kracher, K. Dennis, D. Abanoz, and M. J. Kramer, Philos. Mag. B **82**, 1089 (2002).
[19] J. Dolinšek, M. Klanjšek, T. Apih, A. Smontara, J. C. Lasjaunias, J. M. Dubois, and S. J. Poon, Phys. Rev. B **62**, 8862 (2000).
[20] E. S. Zijlstra and S. K. Bose, Mater. Res. Soc. Symp. Proc. **805**, 135 (2004).
[21] A. Quandt and V. Elser, Phys. Rev. B **61**, 9336 (2000).
[22] E. S. Zijlstra, S. K. Bose, M. Klanjšek, P. Jeglič, and J. Dolinšek, Phys. Rev. B **72**, 174206 (2005).
[23] X. Gonze, J.-M. Beuken, R. Caracas, F. Detraux, M. Fuchs, G.-M. Rignanese, L. Sindic, M. Verstraete, G. Zerah, F. Jollet *et al.*, Comput. Mater. Sci. **25**, 478 (2002); the ABINIT computer program is a common project of the Université Catholique de Louvain, Corning Incorporated, and other contributors (URL: http://www.abinit.org).
[24] Y. Yamamoto, H. Takakura, T. Ozeki, A. P. Tsai, and Y. Ohashi, J. Non-Cryst. Solids **334**, 151 (2004).
[25] K. Schwarz, P. Blaha, and G. K. H. Madsen, Comput. Phys. Commun. **147**, 71 (2002); we used version 3 of the WIEN2k program. We did not use the symmetry of the space group *Cm* (No. 8) of the modified Quandt-Elser model because of a known bug in the implementation of this symmetry. Instead, we specified all atomic positions separately and used space group *P1* (No. 1), which assumes no symmetries besides lattice periodicity.
[26] W. Kohn and L. J. Sham, Phys. Rev. **140**, A1133 (1965).
[27] J. P. Perdew and Y. Wang, Phys. Rev. B **45**, 13244 (1992).
[28] G. K. H. Madsen, P. Blaha, K. Schwarz, E. Sjöstedt, and L. Nordström, Phys. Rev. B **64**, 195134 (2001).
[29] D. Singh, Phys. Rev. B **43**, 6388 (1991).
[30] M. Klanjšek, P. Jeglič, P. McGuiness, M. Feuerbacher, E. S. Zijlstra, J. M. Dubois, and J. Dolinšek, Phys. Rev. B **68**, 134210 (2003).
[31] M. Krajčí and J. Hafner, Phys. Rev. B **59**, 8347 (1999).
[32] M. Krajčí and J. Hafner, Europhys. Lett. **63**, 63 (2003).
[33] *International Tables for Crystallography*, Vol. A, 3rd ed., edited by T. Hahn, Space-Group Symmetry (Kluwer Academic Publishers, Dordrecht, 1992).